LABORATORY STUDIES ON THE FORMATION OF THREE C_2H_4O ISOMERS—ACETALDEHYDE (CH_3CHO), ETHYLENE OXIDE (c-C_2H_4O), AND VINYL ALCOHOL (CH_2CHOH)—IN INTERSTELLAR AND COMETARY ICES

CHRIS J. BENNETT,[1] YOSHIHIRO OSAMURA,[2] MATT D. LEBAR,[1] AND RALF I. KAISER[1,3,4]

ABSTRACT

Laboratory experiments were conducted to unravel synthetic routes to form three C_2H_4O isomers—acetaldehyde (CH_3CHO), ethylene oxide (c-C_2H_4O), and vinyl alcohol (CH_2CHOH)—in extraterrestrial ices via electronic energy transfer processes initiated by electrons in the track of MeV ion trajectories. Here we present the results of electron irradiation on a 2:1 mixture of carbon dioxide (CO_2) and ethylene (C_2H_4). Our studies suggest that suprathermal oxygen atoms can add to the carbon-carbon π bond of an ethylene molecule to form initially an oxirene diradical (addition to one carbon atom) and the cyclic ethylene oxide molecule (addition to two carbon atoms) at 10 K. The oxirene diradical can undergo a [1, 2]-H shift to the acetaldehyde molecule. Both the ethylene oxide and the acetaldehyde isomers can be stabilized in the surrounding ice matrix. To a minor amount, suprathermal oxygen atoms can insert into a carbon-hydrogen bond of the ethylene molecule, forming vinyl alcohol. Once these isomers have been synthesized inside the ice layers of the coated grains in cold molecular clouds, the newly formed molecules can sublime as the cloud reaches the hot molecular core stage. These laboratory investigations help to explain astronomical observations by Nummelin et al. and Ikeda et al. toward massive star-forming regions and hot cores, where observed fractional abundances of these isomers are higher than can be accounted for by gas-phase reactions alone. Similar synthetic routes could help explain the formation of acetaldehyde and ethylene oxide in comet C/1995 O1 (Hale-Bopp) and also suggest a presence of both isomers in Titan's atmosphere.

Subject headings: astrobiology — astrochemistry — comets: general — ISM: molecules — methods: laboratory — molecular processes — planets and satellites: individual (Titan)

Online material: color figure

1. INTRODUCTION

The interstellar medium—the vast space between the stars—contains about 10% of the mass of our Galaxy and consists of gas (99%) and submicrometer-sized grain particles (1%) with averaged number densities of 1 H atom cm^{-3} and 10^{-11} grains cm^{-3}, respectively (Pendleton 1997; Ehrenfreund et al. 1998; Minh & van Dishoeck 2000; Kaiser 2002; Draine 2003). The chemical composition of the interstellar medium is dominated by neutral hydrogen (93.38%) and helium (6.49%), whereas the main biogenic elements oxygen, carbon, and nitrogen contribute 0.11% (O:C:N $\approx$ 8:4:1; Hartquist & Williams 1998). This elementary classification is well reflected in the molecular composition of interstellar space. Molecules, radicals, and ions are ubiquitous in extraterrestrial environments—to date over 130 molecular species have been observed[5] with great diversity, ranging from small molecules like hydrogen (H_2) to astrobiologically important species such as the sugar glycolaldehyde (Hollis et al. 2000) and the amino acid glycine (Kuan et al. 2003). Of the molecules observed so far, groups of isomers (molecules with the same chemical formula but with different connections of the atoms) have received special attention, as the relative abundances of structural isomers will depend strongly on the physical and chemical conditions such as temperature, pressure, radiation sources, and molecular

composition of the interstellar medium. Therefore, isomers can act as tracers to elucidate temperature and density-dependent formation routes to synthesize complex interstellar molecules. In addition, further insights can be gained into the astrochemical evolution of cold molecular clouds, hot molecular cores, and star-forming regions, which are known to be strongly dependent on the molecular composition (Williams & Hartquist 1999; Millar 2002; Charnley & Markwick 2003; Price et al. 2003; Rodgers & Charnley 2003; Wiebe et al. 2003). Thus, it is of paramount importance to unravel the basic physical and chemical processes of how complex molecules are actually formed in these environments.

A detailed understanding of the formation of three C_2H_4O isomers—these are acetaldehyde (CH_3CHO), ethylene oxide (c-C_2H_4O), and vinyl alcohol (H_2CCHOH) (Fig. 1)—is of particular pertinence to test the astrochemical evolution of the interstellar medium, since these molecules also play a key role in astrobiology (Hjalmarson et al. 2001; Turner & Apponi 2001; Charnley 2004; Kuan et al. 2004). For example, acetaldehyde and ethylene oxide have been suggested to play an important function in amino acid formation (Cleaves 2003) and early metabolic pathways (Miller & Schlesinger 1993), respectively. Furthermore, the presence of ethylene oxide suggests the possible presence of a larger ring structure, furan (c-C_4H_4O), to which the sugars ribose and deoxyribose are closely related; these molecules linked by phosphate(s) make up the structural backbone in RNA and DNA, respectively (Hjalmarson et al. 2001).

Acetaldehyde is ubiquitous in the interstellar medium and has been observed in three types of interstellar environments: (1) in translucent clouds such as CB 17, CB 24, and CB 228 at a surprisingly high fractional abundance of $\approx 1 \times 10^{-8}$, although the authors note this may be a factor of 10 too high (Turner et al. 1999); (2) in cold molecular clouds such as the Taurus Molecular

[1] Department of Chemistry, University of Hawai'i at Manoa, Honolulu, HI 96822.
[2] Department of Chemistry, Rikkyo University, 3-34-1 Nishi-ikebukuro, Tokyo, 171-8501, Japan.
[3] Department of Physics and Astronomy, The Open University, Milton Keynes MK7 6AA, UK.
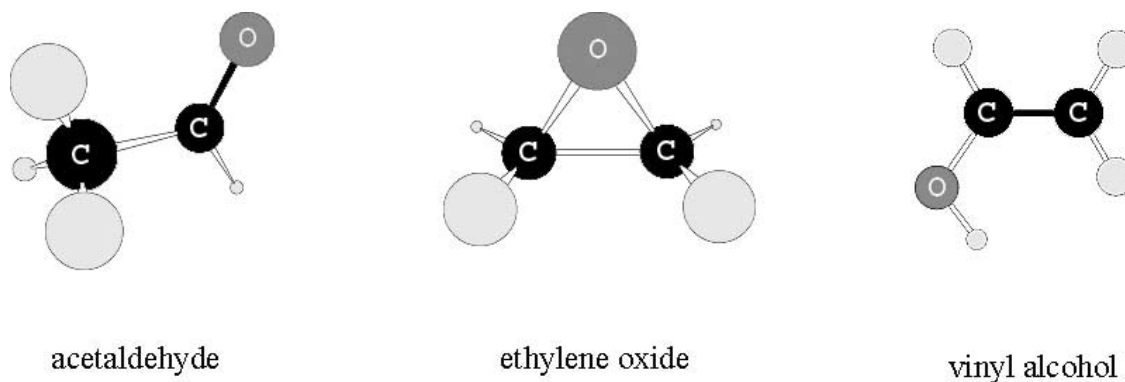[4] Corresponding author: kaiser@gold.chem.hawaii.edu.
[5] See http://www.cv.nrao.edu/~awootten/allmols.html.

Fig. 1.—Structures of three C$_2$H$_4$O isomers: acetaldehyde, ethylene oxide, and vinyl alcohol (most stable cis conformer shown). [*See the electronic edition of the Journal for a color version of this figure.*]

Cloud (TMC-1) and L134N with fractional abundances of between about 10^{-10} and 10^{-9} (Matthews et al. 1985; Turner et al. 1999); and (3) toward hot cores and star-forming regions like Sgr B2N, NGC 6334F, and the Orion Compact Ridge with fractional abundances varying from about 10^{-11} to 3×10^{-9} (Fourikis et al. 1974; Bell et al. 1983; Turner 1991; Ziurys & McGonagle 1993; Nummelin et al. 1998; Ikeda et al. 2001; Charnley 2004). Ethylene oxide has so far only been identified toward hot cores, including Sgr B2N and NGC 6334F at fractional abundances from 2×10^{-12} to 6×10^{-10} (Dickens et al. 1997; Nummelin et al. 1998; Ikeda et al. 2001). It should be noted that the most recent survey observing the abundances of acetaldehyde and ethylene oxide within hot cores by Ikeda et al. (2001) showed acetaldehyde commonly in excess within the ratios of 1.2–13.2, where the lowest reported ratio is for Sgr B2N. Vinyl alcohol has only recently been identified in the hot core Sgr B2N at a fractional abundance of 4×10^{-11} and thus represents the only interstellar environment where all three isomers have been observed (Turner & Apponi 2001). The ratios often reported for these isomers are given as $1:1.5:1$ (CH$_3$CHO : c-C$_2$H$_4$O : CH$_2$CHOH). However, there remains a large uncertainty in the abundance of acetaldehyde within this source; the ratios of the weaker to stronger absorption lines observed by Turner (1991) were inconsistent (too high) for an optically thin source. Thus, he suggested a possible correction factor that would set the ratios possibly as high as $800:1.5:1$. Using the alternative values from Ikeda et al. (2001), the ratios are given as $2:1.5:1$, but the authors did not comment on the validity of the observed acetaldehyde abundance in this source.

Despite the importance of these isomers, their formation routes in the interstellar medium have not been resolved yet. A reaction for formation of acetaldehyde at low temperatures in the gas phase was proposed by Smith & Adams (1977; Huntress & Mitchell 1979). The radiative association reaction forming the protonated acetaldehyde cation,

$$CH_3^+ + H_2CO \rightarrow CH_3CHOH^+ + h\nu, \qquad (1)$$

followed by the dissociative recombination process,

$$CH_3CHOH^+ + e^- \rightarrow CH_3CHO + H, \qquad (2)$$

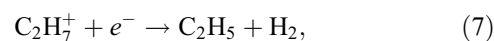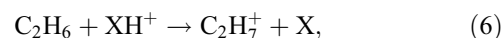was suggested to produce acetaldehyde. Alternatively, Leung et al. (1984) proposed a mechanism that forms the protonated acetaldehyde cation via

$$HCO^+ + CH_4 \rightarrow CH_3CHOH^+, \qquad (3)$$

followed by the same dissociative recombination step as before (reaction [2]; Huntress & Mitchell 1979). A third gas-phase route was speculated to proceed via the reaction sequence

$$CH_5^+ + H_2CO \rightarrow CH_3CHOH^+ + H_2, \qquad (4)$$

$$CH_5^+ + CO \rightarrow CH_3CHOH^+ + h\nu, \qquad (5)$$

again followed by step (2) (Huntress & Mitchell 1979; Leung et al. 1984). Finally, Charnley et al. (1992) suggest the gas-phase reaction sequence

$$C_2H_6 + XH^+ \rightarrow C_2H_7^+ + X, \qquad (6)$$

$$C_2H_7^+ + e^- \rightarrow C_2H_5 + H_2, \qquad (7)$$

$$C_2H_5 + O \rightarrow CH_3CHO + H; \qquad (8)$$

the first step is the protonation of ethane (reaction [6]), which then undergoes dissociative recombination to C$_2$H$_5$—presumably forming molecular hydrogen as the second product (reaction [7])—which can then undergo a then neutral-neutral reaction with oxygen to form acetaldehyde and a hydrogen atom (reaction [8]). Regarding ethylene oxide, Dickens et al. (1997) cite a 1997 private communication from E. Herbst in which two mechanisms for the formation of ethylene oxide were presented. The first mechanism is the neutral-neutral reaction of atomic oxygen with the ethyl radical in the gas phase (similar to reaction [8]). The second formation pathway could be the combination of the two reactions (Caselli et al. 1993; Dickens et al. 1997)

$$CH_3^+ + C_2H_5OH \rightarrow C_2H_5O^+ + CH_4, \qquad (9)$$

$$C_2H_5O^+ + e^- \rightarrow c\text{-}C_2H_4O + H. \qquad (10)$$
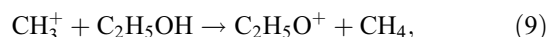
Turner & Apponi (2001) propose that vinyl alcohol is formed along with ethylene oxide via ion-molecule reactions; presumably the actual physical processes occurring would be similar to those stated in reactions (1) and (2):

$$CH_3^+ + H_2CO \rightarrow ? \rightarrow CH_2CHOH + c\text{-}C_2H_4O. \qquad (11)$$

Basiuk & Kobayashi (2004) recently studied theoretically the possible formation of vinyl alcohol via several possible reaction sequences involving simple radical processes of species abundant in the interstellar medium, and similar formation pathways could likely be proposed for the remaining isomers. However,

these processes have not yet been included in models of interstellar environments, and many of the intermediates involved have not yet been observed in the interstellar medium. Experiments performed by Hudson & Moore (2003) suggested that vinyl alcohol can also be formed in the solid phase upon irradiation of $H_2O:C_2H_2$ ices (4:1 ratio) with 0.8 MeV protons and 10.2 eV (121.6 nm) photons via

$$H_2O + C_2H_2 \rightarrow ? \rightarrow H_2CCHOH, \qquad (12)$$

although the reaction mechanism has not been established yet (also not included in models so far). However, theoretical models that simulate the chemical processes of dark molecular clouds and star-forming regions including reactions (1)–(10) could not fit the astronomically observed fractional abundances of all three observed C_2H_4O isomers simultaneously. The majority of the mechanistic information on potential synthetic routes has been derived from pure gas-phase reaction networks in cold molecular clouds (Fairley et al. 1996; El-Nawawy et al. 1997). Assuming a standard cosmic-ray ionization rate of 1×10^{-17} s^{-1}, these models reproduce nicely the observed fractional abundances of acetaldehyde of a few times 10^{-10} in cold clouds like TMC-1. However, to actually explain the increased abundances of acetaldehyde in hot cores compared to cold molecular clouds and the astronomically observed column densities of ethylene oxide and vinyl alcohol in Sgr B2, Millar et al. (1997) simulated these sublimation processes and injected molecules from the solid state into the gas phase to enhance the production of acetaldehyde via gas-phase ion-molecule reactions. Nevertheless, these models could not reproduce the abundances of complex molecules like acetaldehyde and its isomers. Depending on the physical and chemical conditions in the models, molecular abundances are a factor of 100 too high or too low. Charnley (2004) confirmed these deductions and concluded that pure ion-molecule reaction schemes are unlikely to be the origin of C_2H_4O isomers in star-forming regions and also that reaction schemes including neutral-neutral schemes were insufficient to reproduce the abundances of acetaldehyde. A comment should be made that recently, Nomura & Millar (2004) did manage to fairly successfully model the abundance of acetaldehyde (the other isomers were not investigated), which was less than a factor of 2 out from the observed value toward the hot core G34.3+0.15 using reaction (8). As ethane (C_2H_6) is considered to be a required precursor to this reaction, the acetaldehyde concentration would be closely correlated to the amount of ethane present in the environment being modeled, and thus the contribution and validity of this reaction scheme could be investigated.

Alternative scenarios propose a formation of acetaldehyde via grain-surface reactions of hydrogen, carbon, and oxygen atoms in cold molecular clouds through radical-radical, atom-radical, and atom-atom reactions on interstellar grains at 10 K (Charnley et al. 2001; Turner & Apponi 2001; Williams & Herbst 2002; Zhitnikov & Dmitriev 2002; Rae et al. 2003; Charnley 2004), which is then liberated into the gas phase via sublimation in hot cores when the surrounded matter is heated by the embedded protostar (Millar & Hatchel 1998). However, even this refined model could not fit observed abundances of acetaldehyde. Recently, Ruffle & Herbst (2001) and Stantcheva et al. (2001) incorporated effects of surface photochemistry in quiescent dense cores into a combined gas-phase and grain-surface model. Although this approach did not investigate the formation of acetaldehyde explicitly, the authors concluded that the inclusion of these processes only slightly increases molecular abundances and that grain-surface photochemistry has only a minor role because of the small ultraviolet photon flux and the mitigating effect of hydrogen atoms. Here, atomic hydrogen migrates more rapidly than any other atom or radical on the 10 K grain surfaces, thus saturating the free valences of radical intermediates and inhibiting the formation of complex organic molecules, and consequently those formed on grain surfaces are likely to be completely saturated by hydrogen atoms (acetaldehyde and vinyl alcohol are not).

These considerations make it exceptionally clear that neither gas-phase ion-molecule reactions nor grain-surface processes can explain the enhanced abundances of acetaldehyde in star-forming regions, typically of up to a few times 10^{-9}; likewise, synthetic routes to form ethylene oxide and vinyl alcohol in hot cores remain elusive. Therefore, we have to conclude that key production routes to form the C_2H_4O isomers in hot molecular cores are still missing. The crucial drawback of currently existing chemical reaction networks is that the material inside the nanometer-thick ice mantles of grains in molecular clouds is assumed to be chemically inert at 10 K, composed of predominantly water (H_2O), methanol (CH_3OH), carbon monoxide (CO), carbon dioxide (CO_2), and minor components such as ammonia (NH_3), formaldehyde (H_2CO), hydrogen cyanide (HCN), carbonyl sulfide (OCS), and methane (CH_4) (Fraser et al. 2002; Ehrenfreund & Schutte 2000; Gibb et al. 2004). This assumption limits the validity of grain-surface models significantly, since the chemical evolution of interstellar and cometary ices by bombardment with broadband ultraviolet photons (Gerakines et al. 1996; Allamandola et al. 1999; Dartois et al. 1999; Schutte 1998; Bernstein et al. 2002; Muñoz Caro & Schutte 2003) and MeV cosmic-ray and keV solar wind particles is well established (Johnson 1990, 1996; Brucato et al. 1997; Kaiser & Roessler 1997, 1998; Smith 1997; Lécluse et al. 1998; Strazzulla & Palumbo 1998; Hudson & Moore 1999; Kaiser et al. 1999; Palumbo et al. 1999, 2000; Gerakines et al. 2004). Therefore, in photon-shielded, dark molecular clouds the pristine ice mantles can be processed chemically by the high-energy cosmic radiation field. Once complex molecules such as acetaldehyde, ethylene oxide, and vinyl alcohol have been formed *inside* ices, the inherent temperature increase from 10 K to up to 200 K that goes along with transition from the cold molecular cloud to the hot core phase could lead to a sublimation of the newly formed molecules into the gas phase.

2. OBJECTIVES

The prime directive of our research is to investigate experimentally the formation of interstellar acetaldehyde and its isomers ethylene oxide and vinyl alcohol in interstellar ices via charged particles of the cosmic-ray radiation field and to carry out experiments under well-defined physicochemical conditions that simulate the high-energy particle component, the temperatures, and the chemical composition of cold molecular clouds and hot cores in an ultrahigh vacuum scattering machine. With respect to the chemical composition, it should be noted that in order to resolve the formation pathways of complex molecules occurring within these ices, it is a necessary prerequisite to understand the irradiation effects on pure ices and also on binary mixtures before studying more complicated and more astrophysically relevant ice mixtures. We have demonstrated previously that a simple carbon-hydrogen σ-bond rupture in methane (CH_4)–carbon monoxide (CO) ice mixtures upon electron irradiation at 10 K can indeed form acetaldehyde molecules (Bennett et al. 2005; Fig. 2, *top*). However, neither ethylene oxide nor vinyl alcohol was detected in this system. Here, we expand these studies and attempt to elucidate whether the reaction of suprathermal oxygen atoms inside ices—generated via electronic energy transfer processes from
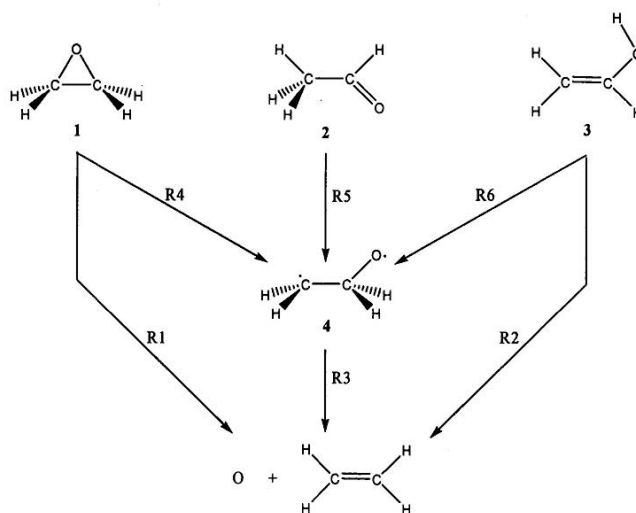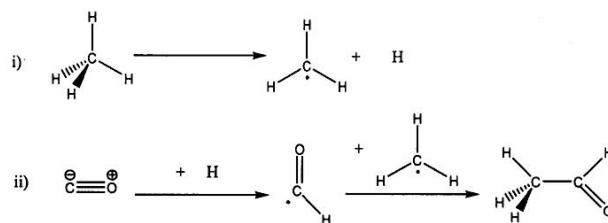
Fig. 2.—Synthetic routes to acetaldehyde in carbon monoxide–methane ices (*top, routes i and ii*) to ethylene oxide (*species 1*), acetaldehyde (*species 2*), and vinyl alcohol (*species 3*) in the oxygen-ethylene system (*bottom*; spin states are omitted for clarity). Synthetic routes are derived combining concepts of suprathermal chemistry (Roessler 1992; Kaiser 2002; Bennett et al. 2005) together with a classical retrosynthetic approach (Smith & March 2001).

energetic electrons (called δ electrons) in the ultra track of MeV cosmic-ray protons and helium nuclei (Bennett et al. 2004, 2005)—with ethylene molecules (C_2H_4) can access the C_2H_4O potential energy surface to form acetaldehyde, ethylene oxide, and/or vinyl alcohol (Fig. 2, *bottom*). Sequentially going through these pathways, reaction R1 describes the formation of ethylene oxide (species 1) via addition of the oxygen atom across the $C = C$ double bond (π bond) of the ethylene molecule. Reaction R2 represents the insertion process of an oxygen atom into the $C-H$ bond (σ bond) to give vinyl alcohol (species 3). The oxirane diradical (species 4) formed by the addition of the oxygen atom to a single carbon atom of the π bond (reaction R3) signifies a possible intermediate that may be isolated should any of the remaining reactions occur, which are the subsequent ring closure to species 1 (reaction R4) or the migration of a hydrogen atom from the central carbon atom to either the second carbon atom yielding acetaldehyde (species 2; reaction R5) or the oxygen atom to give species 3 (reaction R6). Both reactions R1 and R2 are "one-step" processes, whereas reactions R4–R6 depend on the prior formation of species 4 and are therefore "two-step" processes. There is also the possibility of reactions occurring from the generation and subsequent recombination of radicals (including hydrogen abstraction reactions), which we address in the discussion. We would like to point out that these reactions can proceed either on the triplet surface (the reacting oxygen atom is in its ^3P_j ground state) or on the singlet surface (if the atomic oxygen reactant is in its first electronically excited ^1D state); intersystem crossing might complicate the scenario. Based on these considerations, the reactions of oxygen atoms—liberated by cosmic-ray particles from oxygen-bearing molecules in ices,

such as carbon dioxide (also carbon monoxide or water)—with ethylene might form acetaldehyde, ethylene oxide, and/or vinyl alcohol simultaneously.

However, to actually design simulation experiments, we have to compare these reactants with those molecules actually observed in interstellar ices. A recent *Infrared Space Observatory* (*ISO*) survey along the line of sight of 23 young stellar objects (required for a background infrared source, as only absorption features can be detected) indicated the presence of carbon dioxide within ices at abundances between 7% and 35% relative to water (Ehrenfreund et al. 1996; d'Hendecourt et al. 1999; Schutte 1998; Gibb et al. 2004). Note that ethylene has not been observed so far on interstellar grains. Nevertheless, laboratory experiments showed that ethylene can be formed in methane-rich ices via suprathermal chemistry (Kaiser & Roessler 1998); the actual ethylene abundance in interstellar ices is therefore likely to be less than 1% and, hence, not detectable with existing telescopes. Methane, however, is present in ices toward the protostellar objects W33A (1.9%), RAFGL 7009S (4%), and GCS 4 (<17%) (Sandford et al. 1988; Boogert et al. 1996, 1997, 1998; Ehrenfreund et al. 1997; Gibb et al. 2000, 2004; Keane et al. 2001). Note that both carbon dioxide (6%–30%) and methane (0.7%) have been also detected in cometary ices (Crovisier 1998). Although, again, ethylene has not yet been detected in comets, Crovisier et al. (2004) recently published a paper indicating upper limits for some molecular species in comet C/1995 O1 (Hale-Bopp), which included abundances for both acetaldehyde (0.025%) and ethylene oxide (<0.2%) relative to water. These reflections suggest that a CO_2/C_2H_4 binary ice mixture is a likely starting point to address the question of whether acetaldehyde, ethylene oxide, and/or

vinyl alcohol can be formed upon interaction with energetic δ electrons. We would like to emphasize again that no ices that contain solely carbon dioxide and ethylene have been identified so far. The choice of this ice mixture mimics rather neighboring $CO_2-C_2H_4$ molecules in astrophysically relevant ices to address specific mechanisms and generalized concepts on a high-energy induced formation of acetaldehyde, ethylene oxide, and vinyl alcohol in these ices. These data will also help to provide synthetic routes to form C_2H_4O isomers in cold molecular clouds and hot cores—with potential ties to cometary ices.

This paper is organized as follows. The details of the experimental procedures and apparatus and the theoretical approach are outlined in §§ 3 and 4. Synthetic routes to form the C_2H_4O isomers are extracted from the experimental data (§ 5) and are discussed in § 6. The astrophysical implications and a summary (§ 7) conclude this paper.

3. EXPERIMENTAL SECTION

The experiments were conducted in an ultrahigh vacuum (UHV) chamber, which is described in Bennett et al. (2004) in detail. Briefly, the setup consists of a cylindrical stainless steel chamber that can be evacuated down to 8×10^{-11} torr by a magnetically suspended turbomolecular pump backed by an oil-free scroll pump. A closed-cycle helium refrigerator—interfaced to a differentially pumped rotary feedthrough—holds a polished silver monocrystal. The latter serves as a substrate for the ice condensate. The ice condensation is assisted by a precision leak valve that is connected to a gas reservoir. The carbon dioxide (CO_2)–ethylene (C_2H_4) frosts were prepared at about 11 K by depositing premixed gases ($CO_2/C_2H_4 = 4:1$) for 5 minutes at a pressure of 10^{-7} torr onto the cooled silver crystal. Blank checks of the pure gases (C_2H_4, 99.99%; CO_2, 99.9999%) via a quadrupole mass spectrometer and of the ices via a Fourier transform infrared (FTIR) spectrometer showed no traces of any C_2H_4O isomer contamination. Table 1 compiles the absorptions as seen in the infrared spectrum of the frosts prior to the irradiation. To determine the ice composition quantitatively, we integrated various absorption features and calculated the column density, i.e., the number of absorbing molecules per cm^2 inside the ice, via a modified Beer-Lambert relationship (Bennett et al. 2004). These data suggest a CO_2/C_2H_4 ratio of 2.0 ± 0.3 to 1 with column densities of $(1.02 \pm 0.06) \times 10^{18}$ cm^{-2} and $(5.03 \pm 0.72) \times 10^{17}$ cm^{-2} for carbon dioxide and ethylene, respectively (absorption coefficients for CO_2 taken from Gerakines et al. [1995] and for C_2H_4 from Bohn et al. [1994], with the exception of ν_6, for which a value of 7.1×10^{-20} cm molecule^{-1} was estimated from the relative peak areas). Considering densities of 0.8 g cm^{-3} (C_2H_4 ice) and of 1.6 g cm^{-3} (CO_2 ice) at 10 K (Donnay & Ondik 1972), this translates into a target thicknesses of 0.29 ± 0.04 μm of ethylene and 0.47 ± 0.03 μm of carbon dioxide ices. This procedure is accurate to within $\pm 10\%$ (Kaiser et al. 1995). Dynamic simulations of this ice mixture using the CASINO code (Drouin et al. 2001) suggest that each 5 keV electron is fully absorbed within the ice sample within 600 nm, resulting in the transfer of all of its kinetic energy to the ice matrix. (The linear energy transfer [LET] is therefore estimated to be around 8 keV μm^{-1}.)

The samples were irradiated isothermally at 10 K with 5 keV electrons generated with an electron gun (Specs EQ 22–35) at beam currents of 100 nA for 30 minutes by scanning the electron beam over an area of 3.0 ± 0.4 cm^2. In theory, this would mean that during the irradiation the sample would be exposed to 1.1×10^{15} electrons (3.8×10^{14} electrons cm^{-2}); however, not all of the electrons generated by our electron gun actually reach the

TABLE 1
INFRARED ABSORPTIONS OF THE CARBON DIOXIDE–ETHYLENE FROST AND ASSIGNMENT OF THE OBSERVED BANDS

Frequency (cm^{-1})	Assignment	Characterization
1382	CO_2 ν_1	Symmetric stretch
650	CO_2 ν_2	Out-of-plane bend
2325	CO_2 ν_3	Asymmetric stretch
2278	$^{13}CO_2$ ν_3	Isotope peak
1276	CO_2 $2\nu_2$	Overtone
3700	CO_2 $\nu_1 + \nu_3$	Combination
3594	CO_2 $2\nu_2 + \nu_3$	Combination
3010	C_2H_4 ν_1	CH_2 symmetric stretch
1618	C_2H_4 ν_2	CC stretch
1340	C_2H_4 ν_3	CH_2 scissors
3071	C_2H_4 ν_5	CH_2 asymmetric stretch
1227	C_2H_4 ν_6	CH_2 rock
960	C_2H_4 ν_7	CH_2 wag
3096	C_2H_4 ν_9	CH_2 asymmetric stretch
826	C_2H_4 ν_{10}	CH_2 rock
2979	C_2H_4 ν_{11}	CH_2 symmetric stretch
1440	C_2H_4 ν_{12}	CH_2 scissors

NOTE.—Assignment according to Gerakines et al. (1995) for carbon dioxide and Shimanouchi (1972) for ethylene.

target—the manufacturer states an extraction efficiency of 78.8%, meaning the actual number of electrons that hit the sample is reduced to 8.9×10^{14} electrons (3.0×10^{14} electrons cm^{-2}). To guarantee an identification of the reaction products in the ices, they were analyzed with an FTIR spectrometer online and in situ. The chemical modifications of the ice targets are monitored during the experiments to extract time-dependent concentration profiles and hence production rates of newly formed molecules and radicals in the solid state via a Nicolet 510 DX FTIR spectrometer (6000–500 cm^{-1}) operating in an absorption-reflection-absorption mode (reflection angle $\alpha = 75°$). The infrared beam is coupled via a mirror flipper outside the spectrometer, passes through a differentially pumped potassium bromide (KBr) window, is attenuated in the ice sample prior to and after reflection at a polished silver wafer, and exits the main chamber through a second differentially pumped KBr window before being monitored using a liquid-nitrogen–cooled detector (mercury-cadmium-telluride detector type B).

4. THEORETICAL SECTION

We have examined the structures and energetics of acetaldehyde, ethylene oxide, and vinyl alcohol in terms of ab initio molecular orbital methods employing the hybrid density functional B3LYP method (Lee et al. 1988; Becke 1993) with the 6-311G(d,p) basis functions in order to optimize the molecular structures at the energy minima. The relative energies were then refined by using the coupled cluster CCSD(T) method (Purvis & Bartlett 1982; Raghavachari et al. 1989) with the aug-cc-pVTZ basis functions (Dunning 1989) at the structures obtained by the B3LYP method. All relative energies were corrected by the zero-point vibrational energies calculated with the B3LYP method without scaling. All calculations were carried out with the GAUSSIAN 98 program package (Frisch et al. 2001). In order to analyze the infrared spectra for the species obtained by the present experiments, we have calculated the vibrational frequencies and infrared intensities for the structures obtained with the B3LYP/6-311G(d,p) method (Table 2). For the purpose of consistency, we use the calculated intensity values derived here at the same level of theory

TABLE 2

Vibrational Frequencies and Integral Absorption Coefficients

Band	Characterization	Frequency (cm^{-1})	A (cm molecule^{-1})
CH$_3$CHO ($X\,^1A'$)			
ν_1 (a')........	CH$_3$ asymmetric stretching	3073	2.0×10^{-18}
ν_2 (a')........	CH$_3$ symmetric stretching	2961	5.0×10^{-19}
ν_3 (a')........	CH stretching	2798	2.4×10^{-17}
ν_4 (a')........	CO stretching	1788	3.0×10^{-17}
ν_5 (a')........	CH$_3$ deformation	1431	3.7×10^{-18}
ν_6 (a')........	CH bending	1397	2.0×10^{-18}
ν_7 (a')........	CH$_3$ umbrella	1348	4.5×10^{-18}
ν_8 (a')........	CH$_3$ rocking	1103	4.3×10^{-18}
ν_9 (a')........	C—C stretching	865	1.5×10^{-18}
ν_{10} (a')	CCO bending	498	2.3×10^{-18}
ν_{11} (a'').......	CH$_3$ asymmetric stretching	3014	1.7×10^{-18}
ν_{12} (a'').......	CH$_3$ deformation	1442	2.0×10^{-18}
ν_{13} (a'').......	HCCH torsion	1112	1.7×10^{-19}
ν_{14} (a'').......	CH$_3$ twisting	761	1.7×10^{-19}
ν_{15} (a'').......	CH$_3$ torsion	156	0
c-C$_2$H$_4$O ($X\,^1A_1$)			
ν_1 (a_1)........	CH$_2$ symmetric stretching	3023	2.2×10^{-18}
ν_2 (a_1)........	CH$_2$ scissor	1510	5.0×10^{-19}
ν_3 (a_1)........	CC, CO stretching	1275	2.5×10^{-18}
ν_4 (a_1)........	CH$_2$ umbrella	1120	0
ν_5 (a_1)........	CC, CO stretching	872	1.1×10^{-17}
ν_6 (a_2)........	CH$_2$ asymmetric stretching	3094	0
ν_7 (a_2)........	CH$_2$ rock	1148	0
ν_8 (a_2)........	CH$_2$ deform	1018	0
ν_9 (b_1)........	CH$_2$ asymmetric stretching	3110	1.0×10^{-17}
ν_{10} (b_1)	CH$_2$ deform	1145	6.7×10^{-19}
ν_{11} (b_1)	CH$_2$ rock	802	0
ν_{12} (b_2)	CH$_2$ symmetric stretching	3015	7.3×10^{-18}
ν_{13} (b_2)	CH$_2$ scissor	1475	0
ν_{14} (b_2)	CH$_2$ umbrella	1117	5.0×10^{-19}
ν_{15} (b_2)	CC, CO stretching	827	1.8×10^{-18}
cis-H$_2$C = CHOH ($X\,^1A'$)			
ν_1 (a')........	OH stretching	3726	5.0×10^{-18}
ν_2 (a')........	CH$_2$ asymmetric stretching	3172	1.8×10^{-18}
ν_3 (a')........	CH stretching	3120	1.2×10^{-18}
ν_4 (a')........	CH$_2$ symmetric stretching	3076	1.2×10^{-18}
ν_5 (a')........	CC stretching	1669	2.8×10^{-17}
ν_6 (a')........	CH$_2$ scissor	1420	2.3×10^{-18}
ν_7 (a')........	OH bend	1332	8.3×10^{-19}
ν_8 (a')........	CH bend	1300	1.2×10^{-18}
ν_9 (a')........	CO stretching	1103	3.1×10^{-17}
ν_{10} (a')	CH$_2$ rock	942	2.0×10^{-18}
ν_{11} (a')	OCC bend	482	2.2×10^{-18}
ν_{12} (a'')	CH$_2$ out of plane	978	5.8×10^{-18}
ν_{13} (a'')	CH$_2$ out of plane	808	1.2×10^{-17}
ν_{14} (a'')	CH$_2$ twist	701	0
ν_{15} (a'')	OH torsion	467	1.8×10^{-17}
trans-H$_2$C = CHOH ($X\,^1A'$)			
ν_1 (a')........	CH$_2$ asymmetric stretching	3187	1.3×10^{-18}
ν_2 (a')........	CH$_2$ symmetric stretching	3097	0
ν_3 (a')........	CH stretching	3070	3.8×10^{-18}
ν_4 (a')........	CC stretching	1697	1.6×10^{-17}
ν_5 (a')........	CH$_2$ scissor	1408	1.7×10^{-19}
ν_6 (a')........	CH bend	1322	5.0×10^{-19}
ν_7 (a')........	OH bend	1265	3.8×10^{-17}
ν_8 (a')........	CO stretching	1122	2.5×10^{-18}
ν_9 (a')........	CH$_2$ rock	938	8.3×10^{-18}
ν_{10} (a')	OCC bend	473	6.6×10^{-19}

TABLE 2—Continued

Band	Characterization	Frequency (cm^{-1})	A (cm molecule^{-1})
trans-H$_2$C = CHOH ($X\,^1A'$)			
ν_{11} (a')	CH$_2$ out of plane	957	3.8×10^{-18}
ν_{12} (a'')	CH$_2$ out of plane	828	1.0×10^{-17}
ν_{13} (a'')	CH$_2$ twist	703	3.3×10^{-18}
ν_{14} (a'')	OH torsion	251	1.8×10^{-17}
ν_{15} (a'')	OH stretching	3790	1.4×10^{-17}

NOTES.—Vibrational frequencies and integral absorption coefficients of the C$_2$H$_4$O isomers calculated with B3LYP/6-311G(d,p) method. The vibrational frequencies shown were subject to a scaling factor of 0.98 from comparisons of the results of calculations at this level of theory with experimental results.

for all abundance calculations on the C$_2$H$_4$O isomers, although *some* solid-state data are available; at this level of theory, the calculated intensities are typically accurate to about 20%.

5. RESULTS

5.1. *Qualitative Results*

The infrared spectra here are analyzed in two steps. First, we investigate the new absorptions qualitatively and assign their carriers. Then, these data are fit to calculate production rates of synthesized molecules in units of molecules cm^{-2} (column density). Table 3 and Figures 3–5 compile the effects of the electron bombardment of the binary ice mixtures. A comparison of the pristine sample with the irradiated ices at 10 K depicts novel absorption features of the acetaldehyde (CH$_3$CHO), ethylene oxide (c-C$_2$H$_4$O), and vinyl alcohol (CH$_2$CHOH). Here, the most intense four of the 15 fundamental bands of acetaldehyde could be unambiguously identified at 1723 (ν_4), 1351 (ν_7), 1123 (ν_8), and 758 cm^{-1} (ν_{14}; Figs. 3a–3d). Most of the weaker absorption features are partly obscured by overlapping with other bands (for example, with ethylene). In the case of the position of the ν_{15} fundamental (CCO deformation) at 150 cm^{-1}, it is out of the range of our detector (lower limit: 450 cm^{-1}). These results are in good agreement with previous results, for example, at 1731, 1354, 1121, and 775 cm^{-1} from Hawkins & Andrews (1983) and 1719, 1349, 1122, and 770 cm^{-1} from Schriver et al. (2004).

TABLE 3

New Infrared Absorptions of the Processed Carbon Dioxide–Ethylene Sample

Frequency (cm^{-1})	Species	Assignment	A (cm molecule^{-1})
2140..........	CO	ν_1 (CO stretch)	1.1×10^{-17a}
1723..........	CH$_3$CHO	ν_4 (CO stretch)	3.0×10^{-17}
1351..........	CH$_3$CHO	ν_7 (CH$_3$ symmetric deform)	4.5×10^{-18}
1123..........	CH$_3$CHO	ν_8 (CC stretch)	4.3×10^{-18}
758...........	CH$_3$CHO	ν_{14} (CH bend)	1.7×10^{-19}
1270sh	c-C$_2$H$_4$O	ν_3 (ring stretch)	2.5×10^{-18}
868..........	c-C$_2$H$_4$O	ν_5 (ring deform)	1.1×10^{-17}
1465..........	c-C$_2$H$_4$O	ν_2 (CH$_2$ scissors)	5.0×10^{-19}
1150..........	c-C$_2$H$_4$O	ν_{10} (CH$_2$ deform)	6.7×10^{-19}
1639..........	cis-CH$_2$CHOH	ν_5 (CC stretch)	2.8×10^{-17}

NOTE.—New absorptions of the sample at 10 K after an irradiation time of 30 minutes (see text for details), together with calculated values for the integral absorption coefficients A.
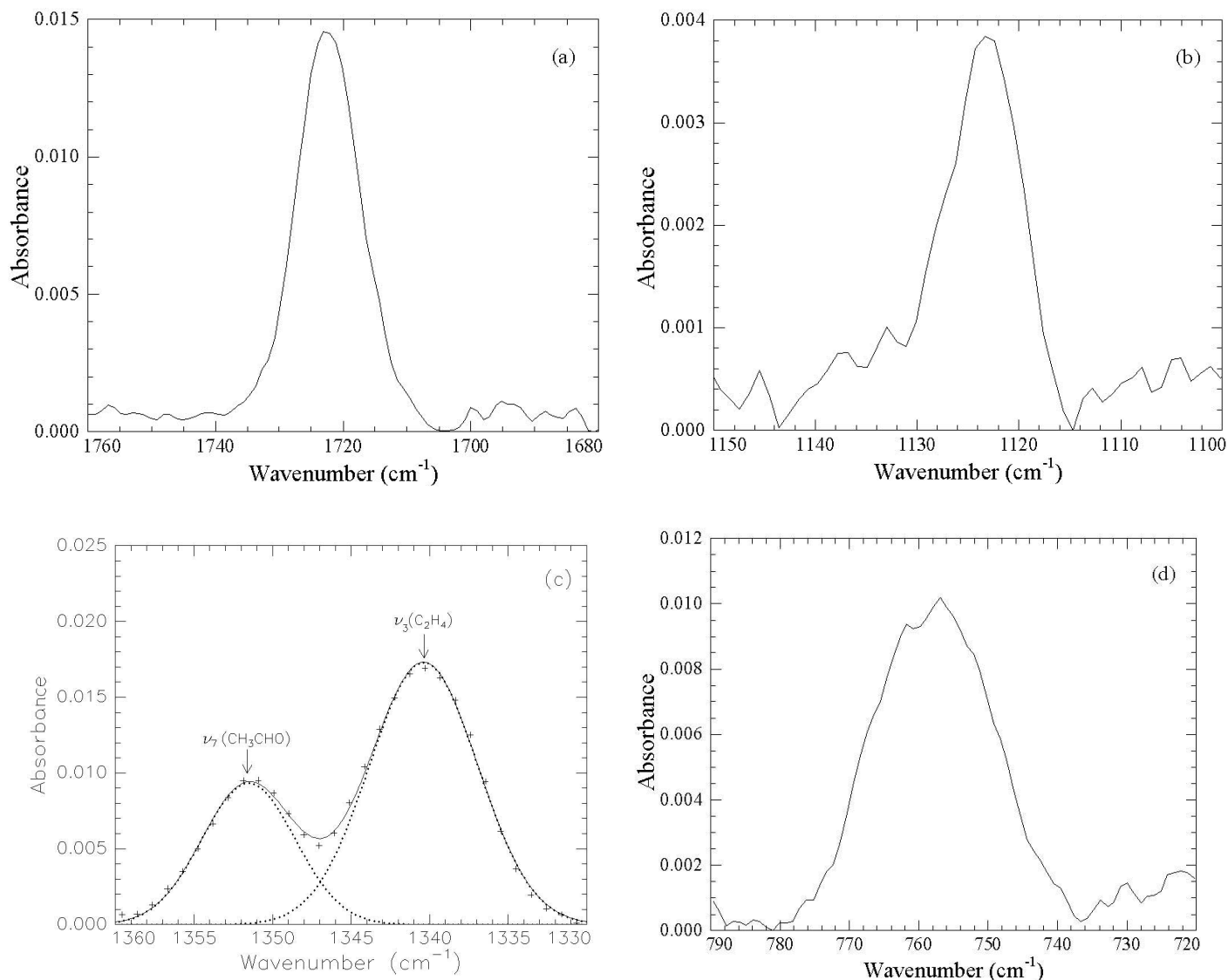
[a] Value from Gerakines et al. (1995).

FIG. 3.—Acetaldehyde absorptions at (*a*) 1723, (*b*) 1124, (*c*) 1351, and (*d*) 757 cm^{-1} as seen after 30 minutes of (100 nA) irradiation of the ice sample at 10 K; the peak at 1340 cm^{-1} has been assigned to the ν_3 fundamental of ethylene.

Considering the case of the cyclic ethylene oxide isomer, we were, for similar reasons, only able to assign the most intense four of the 15 fundamentals unambiguously, at 1270 (ν_3), 868 (ν_5), 1465 (ν_2), and 1150 cm^{-1} (ν_{10}; Figs. 4*a*–4*d*), similar to previous assignments: 1274, 879, 1470, and 1154 cm^{-1} from Hawkins & Andrews (1983) and 1267, 856, 1467, and 1152 cm^{-1} from Schriver et al. (2004). For vinyl alcohol, we assigned only one peak with confidence, namely, the peak at 1641 cm^{-1} (ν_5; Fig. 5), which compares favorably with values of 1631 cm^{-1} (Hawkins & Andrews 1983). Tentative assignments for the more strongly absorbing fundamental (ν_9) could be made to a broader peak at 1077 cm^{-1} as well (cf. 1079 cm^{-1} by Hawkins & Andrews 1983). Comparisons to Hudson & Moore (2003)—studying the formation of this molecule in C_2H_2:H_2O ices—are difficult to make, as the experiments were carried out in a water matrix, which absorbs strongly around 1660 cm^{-1}, thus overlapping with the (ν_5) peak, and the (ν_9) band is shifted to 1145 cm^{-1} due to hydrogen bonding formed with the water matrix. We would like to stress that in this paper, we only focus on the routes to form C_2H_4O isomers. It is necessary to point out for the discussion of the mechanism, however (§ 6), that the formation of the CO fundamental at 2140 cm^{-1} (cf., for example, Gerakines et al. 1995)

was also observed and also that we failed to detect any presence of the vinyl radical (C_2H_3), which absorbs strongly at around 898 cm^{-1} (ν_8; Kaiser & Roessler 1998).

5.2. *Quantitative Analysis*

We investigate now the temporal evolution of the infrared absorptions and the inherent column densities of the synthesized species quantitatively. The development of the column densities of the carbon dioxide and the ethylene reactants is shown in Figures 6 and 7, respectively. We used the absorptions at 3701 and 3595 cm^{-1} to quantify the decay of the carbon dioxide precursor; during the irradiation, the column density decreases from about $(1.02 \pm 0.06) \times 10^{18}$ to $(9.1 \pm 0.6) \times 10^{17}$ molecules cm^{-2}, implying that $(1.1 \pm 0.1) \times 10^{17}$ molecules cm^{-2} (roughly 10%) of the carbon dioxide have been destroyed during the electron exposure. To fit the experimentally obtained profile of the carbon dioxide column density, we presumed that the reactant molecules undergo first-order "decay" upon electron bombardment, similar to a radioactive decay. Therefore, a rate law of

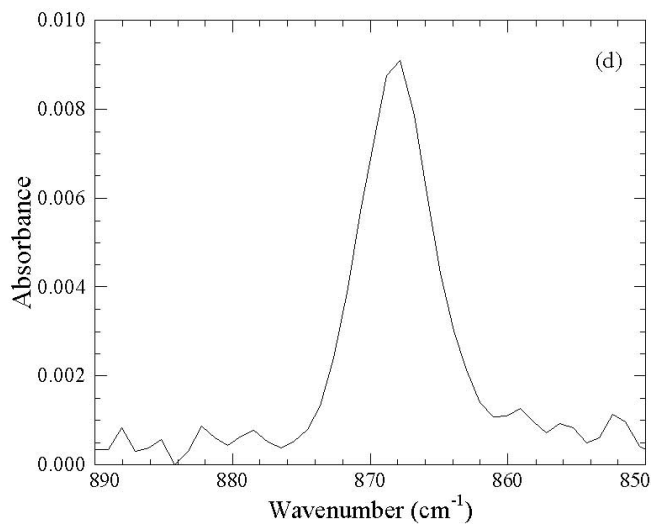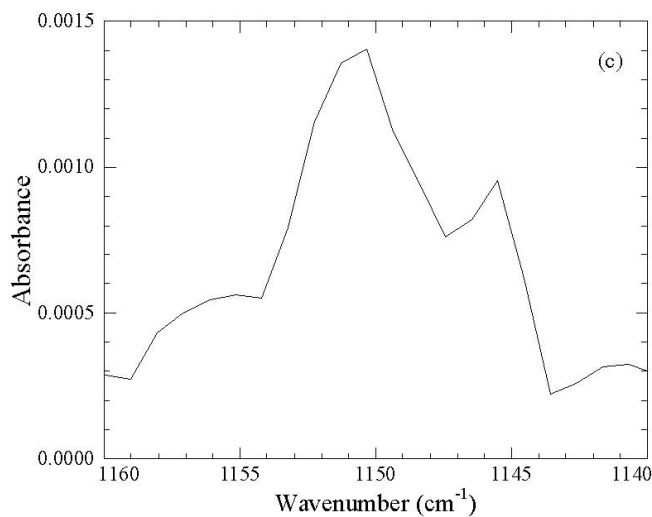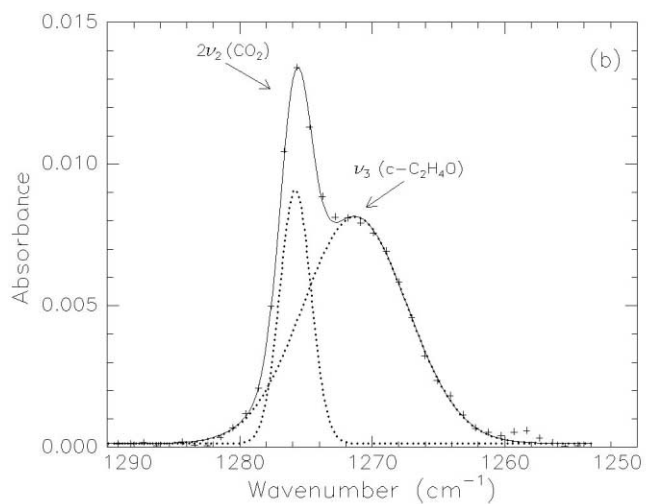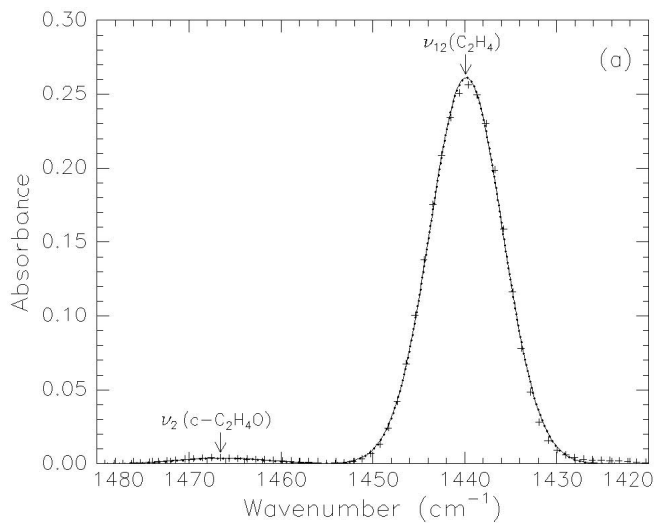$$-d[CO_2]/dt = k_1[CO_2] \qquad (13)$$

Fig. 4.—Ethylene oxide absorptions at (a) 1467, (b) 1271, (c) 1151, and (d) 868 cm^{-1} as seen after 30 minutes of (100 nA) irradiation of the ice sample at 10 K; the peak at 1439 cm^{-1} has been assigned to the ν_{12} fundamental of ethylene in (a); the peak at 1276 cm^{-1} was identified as an overtone of the out-of-plane bending mode of the carbon dioxide.
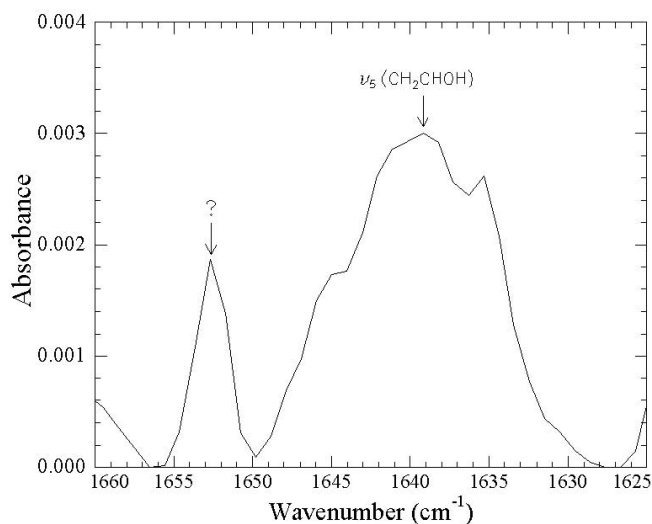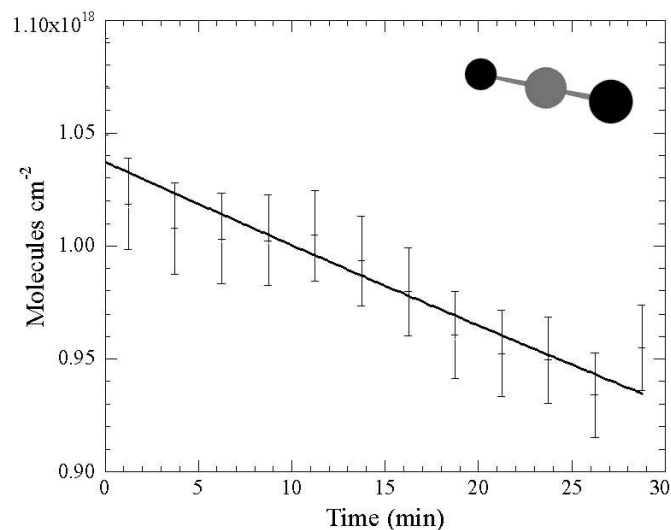

Fig. 5.—Vinyl alcohol absorption at 1639 cm^{-1} as seen after 30 minutes of (100 nA) irradiation of the ice sample at 10 K. The carrier of the peak at 1653 cm^{-1} has not yet been assigned.

Fig. 6.—Fit of the carbon dioxide column densities for the absorption at 3595 cm^{-1}. Error bars show the standard error in the integration of the peak areas ($\sim$2%).
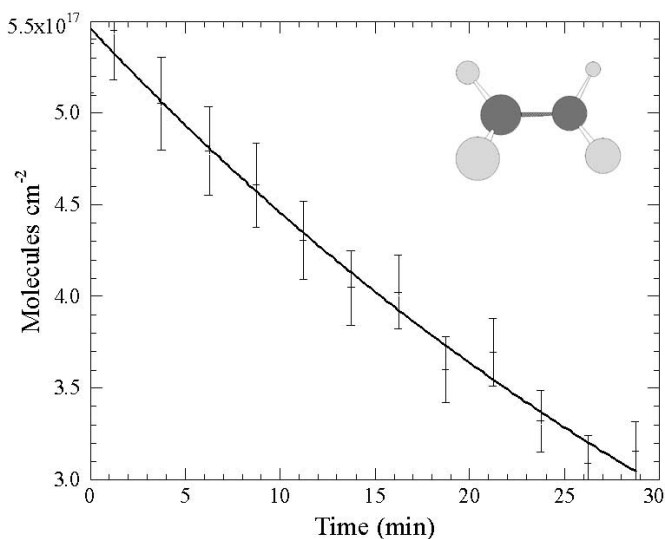
FIG. 7.—Fit of the ethylene column densities for the absorption at 1225 cm^{-1}. Error bars show the standard error in the integration of the peak areas ($\sim$5%).

was used to fit the column density of the carbon dioxide during the irradiation phase via

$$[CO_2](t) = [CO_2](t = 0)e^{-k_1 t}. \qquad (14)$$

The best fits of the temporal profiles yielded $[CO_2](t = 0) = (9.44 \pm 0.90) \times 10^{17}$ molecules cm^{-2} and $k_1 = (5.31 \pm 0.98) \times 10^{-5}$ s^{-1} for the 3701 cm^{-1} feature and $[CO_2](t = 0) = (1.04 \pm 0.01) \times 10^{18}$ molecules cm^{-2} and $k_1 = (6.02 \pm 0.75) \times 10^{-5}$ s^{-1} for the 3595 cm^{-1} feature. A similar approach was used to fit the column densities of the ethylene reactant (Fig. 7) via

$$-d[C_2H_4]/dt = k_2[C_2H_4], \qquad (15)$$

$$[C_2H_4](t) = [C_2H_4](t = 0)e^{-k_2 t}, \qquad (16)$$

where $[C_2H_4](t = 0) = (5.46 \pm 0.06) \times 10^{17}$ molecules cm^{-2} and $k_2 = (3.39 \pm 0.12) \times 10^{-4}$ s^{-1} for the 1225 cm^{-1} feature. Here, averaging over all absorptions investigated during the ir-
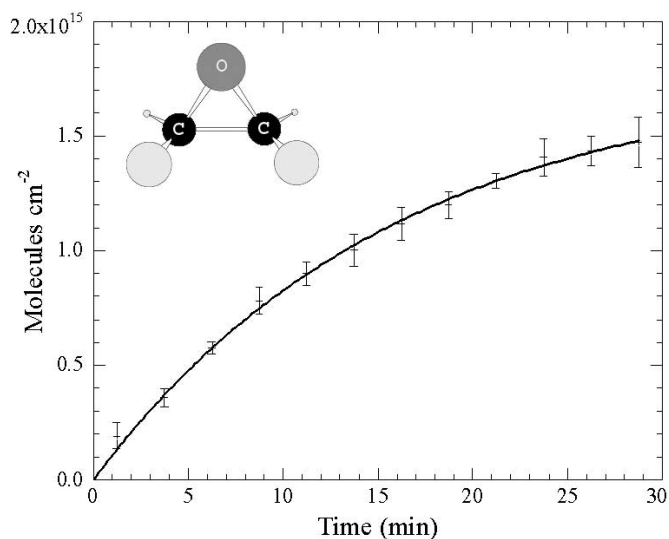

FIG. 9.—Fit of the ethylene oxide column densities for the absorption at 868 cm^{-1}. Error bars show the standard error in the integration of the peak areas.

radiation, the column density of the ethylene reactant reduces from $(5.03 \pm 0.72) \times 10^{17}$ to $(3.85 \pm 0.93) \times 10^{17}$ molecules cm^{-2} by $(1.2 \pm 0.5) \times 10^{17}$ molecules cm^{-2}, i.e., a destruction of about 25% of the ethylene species.

As the column densities of the ethylene and carbon dioxide reactants decline, new features occur from the acetaldehyde, ethylene oxide, and vinyl alcohol (§ 5.1). Here, we were able to fit the experimental data with pseudo–first-order rate laws via

$$[CH_3CHO](t) = a(1 - e^{-k_3 t}), \qquad (17)$$

$$[c\text{-}C_2H_4O](t) = b(1 - e^{-k_4 t}), \qquad (18)$$

$$[CH_2CHOH](t) = c(1 - e^{-k_5 t}). \qquad (19)$$

This procedure yields the best-fit parameters for, e.g., the 1350 cm^{-1} peak of acetaldehyde [$a = (5.75 \pm 0.16) \times 10^{15}$ molecules cm^{-2} and $k_3 = (8.57 \pm 0.43) \times 10^{-4}$ s^{-1}; Fig. 8] and the 868 cm^{-1} peak

FIG. 8.—Fit of the acetaldehyde column densities for the absorption at 1350 cm^{-1}. Error bars of the data are the standard error in the deconvoluted fit of the data.
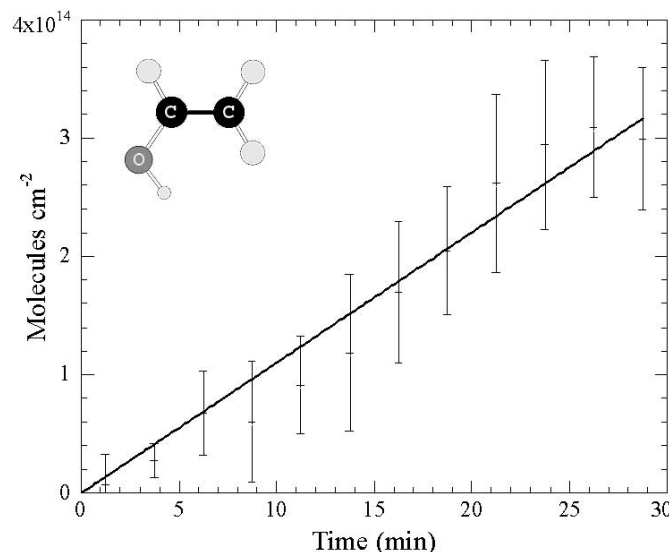

FIG. 10.—Fit of the vinyl alcohol column densities for the absorption at 1639 cm^{-1} using eq. (20). Error bars show the standard error in the integration of the peak areas.
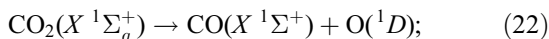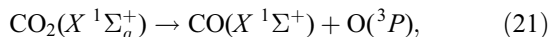
from ethylene oxide [$b = (1.77 \pm 0.05) \times 10^{15}$ molecules cm^{-2} and $k_4 = (1.05 \pm 0.06) \times 10^{-3}$ s^{-1}; Fig. 9]. For the 1639 cm^{-1} peak from vinyl alcohol, we derived

$$[CH_2CHOH](t) \approx ck_5t \qquad (20)$$

based on the approximation $e^x \approx 1 + x$ (i.e., a straight line), which gives $ck_5 = (1.84 \pm 0.06) \times 10^{11}$ cm^{-2} s^{-1} (Fig. 10). The available experimental data do not allow estimating univocally the parameters c and k_5, and further experiments are required. Averaging over all absorptions investigated (Table 2), we calculate $a = (4.0 \pm 2.7) \times 10^{15}$ molecules cm^{-2}, $k_3 = (8.5 \pm 0.3) \times 10^{-4}$ s^{-1}, $b = (4.3 \pm 3.6) \times 10^{15}$ molecules cm^{-2}, and $k_4 = (1.1 \pm 0.1) \times 10^{-3}$ s^{-1}. After the irradiation has finished, column densities of $(3.3 \pm 1.7) \times 10^{15}$, $(4.2 \pm 3.8) \times 10^{15}$, and $(3.0 \pm 0.6) \times 10^{14}$ molecules cm^{-2} of acetaldehyde, ethylene oxide, and vinyl alcohol, respectively, are present. Accounting for the sample area and the number of implanted electrons, about 11 ± 6 acetaldehyde, 14 ± 13 ethylene oxide, and 1 ± 0.2 vinyl alcohol molecules have been synthesized per implanted electron.
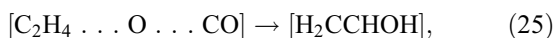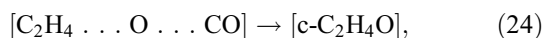
6. DISCUSSION

Considering the formation of the acetaldehyde, ethylene oxide, and vinyl alcohol isomers, our investigations point toward an electron-induced decomposition of the carbon dioxide molecule via

$$CO_2(X\,^1\Sigma_g^+) \rightarrow CO(X\,^1\Sigma^+) + O(^3P), \qquad (21)$$

$$CO_2(X\,^1\Sigma_g^+) \rightarrow CO(X\,^1\Sigma^+) + O(^1D); \qquad (22)$$

this mechanism is identical to the cleavage of a carbon-oxygen double bond, as found in neat carbon dioxide ices (Bennett et al. 2004). Depending on the energy transfer from the electron to the carbon dioxide molecule, the oxygen atom can be generated either in its electronic ground state (^3P) via intersystem crossing to the triplet manifold and/or in its excited state (^1D) on the singlet surface. These processes are found to be endoergic by 532 kJ mol^{-1} (5.51 eV) and 732 kJ mol^{-1} (7.59 eV), respectively.[6] Equations (21) and (22) would suggest an inherent formation of carbon monoxide, as verified experimentally via its absorption at 2140 cm^{-1}. In addition, the decay of the carbon dioxide column densities could be fit through a first-order decay, suggesting a "decomposition" of the carbon dioxide molecule (eqs. [13] and [14]).

To fit the experimentally observed column densities of the acetaldehyde, ethylene oxide, and vinyl alcohol molecules, the following reaction model was investigated:
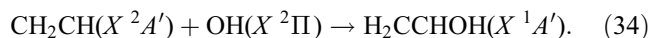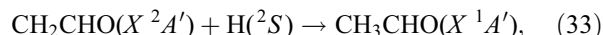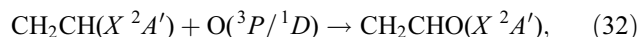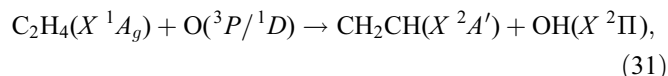
$$[C_2H_4{-}CO_2] \rightarrow [C_2H_4 \ldots O \ldots CO], \qquad (23)$$

$$[C_2H_4 \ldots O \ldots CO] \rightarrow [c\text{-}C_2H_4O], \qquad (24)$$

$$[C_2H_4 \ldots O \ldots CO] \rightarrow [H_2CCHOH], \qquad (25)$$

$$[C_2H_4 \ldots O \ldots CO] \rightarrow [H_2CCH_2O] \rightarrow [c\text{-}C_2H_4O], \qquad (26)$$

$$[C_2H_4 \ldots O \ldots CO] \rightarrow [H_2CCH_2O] \rightarrow [CH_3CHO], \qquad (27)$$

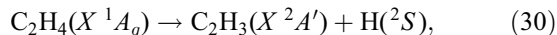$$[C_2H_4 \ldots O \ldots CO] \rightarrow [H_2CCH_2O] \rightarrow [H_2CCHOH]. \qquad (28)$$

Here, the actual reaction is proposed to take place inside a [C$_2$H$_4$—CO$_2$] matrix cage. First, the energy transfer to the carbon dioxide

[6] See http://webbook.nist.gov/chemistry.

molecule releases an oxygen atom to form a [C$_2$H$_4$...O...CO] complex (see Fig. 2; eq. [23]). Hereafter, the oxygen atom adds to the π bond of the ethylene molecule; this process can lead to the formation of the ethylene oxide molecule (species 1 in Fig. 2) in one step through reaction sequence R1 (eq. [24]) via addition to both carbon atoms simultaneously or via addition to only one carbon atom to initially form the oxirane diradical (species 4) via reaction sequence R3, which can subsequently undergo either a ring closure to form ethylene oxide (reaction R4; eq. [26]) or a [1, 2]-H atom shift to form the acetaldehyde species (species 2; reaction R5; eq. [27]), or it could similarly undergo a H atom shift to the oxygen atom to form the vinyl alcohol molecule (species 3; reaction R6; eq. [28]). Alternatively, the oxygen atom can insert into a C—H σ bond to form a vinyl alcohol molecule (species 3; reaction R2; eq. [25]). Depending on the spin state of the oxygen atom, these reactions can take place on the singlet or triplet surface; alternatively, the reaction might start on the triplet surface first, and the intermediates involved can undergo intersystem crossing to the singlet manifold. If the initial reaction of the released oxygen atom with the ethylene molecule and the potentially involved hydrogen migration processes are fast, the temporal profile of the ethylene oxide, acetaldehyde, and vinyl alcohol column densities formed via reactions (23)–(28) should be fit using pseudo–first-order kinetics, as done through equations (17)–(19). We would like to stress that we did not observe any absorptions of the methyl radical, CH$_3$ ($X\,^2A_2''$), or of the formyl species, HCO ($X\,^2A'$). Therefore, a formation of acetaldehyde via a radical-radical recombination,

$$HCO(X\,^2A') + CH_3(X\,^2A_2'') \rightarrow CH_3CHO(X\,^1A'), \qquad (29)$$
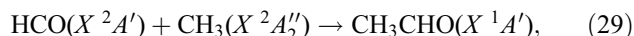
can be clearly ruled out. In addition, due to the failed detection of the vinyl radical C$_2$H$_3$ ($X\,^2A'$), we can rule out the following reactions:

$$C_2H_4(X\,^1A_g) \rightarrow C_2H_3(X\,^2A') + H(^2S), \qquad (30)$$

$$C_2H_4(X\,^1A_g) + O(^3P/^1D) \rightarrow CH_2CH(X\,^2A') + OH(X\,^2\Pi), \qquad (31)$$

$$CH_2CH(X\,^2A') + O(^3P/^1D) \rightarrow CH_2CHO(X\,^2A'), \qquad (32)$$

$$CH_2CHO(X\,^2A') + H(^2S) \rightarrow CH_3CHO(X\,^1A'), \qquad (33)$$

$$CH_2CH(X\,^2A') + OH(X\,^2\Pi) \rightarrow H_2CCHOH(X\,^1A'). \qquad (34)$$

The electron induced decomposition of ethylene would be expected to yield an appreciable amount of the vinyl radical and a hydrogen atom by cleavage of a C—H σ bond (eq. [30]); alternatively, suprathermal oxygen atoms in the ground state (^3P) and excited state (^1D) are known to undergo hydrogen abstraction reactions to yield the vinyl radical plus a hydroxyl radical (eq. [31]). Following the formation of the vinyl radical, it could react without a barrier to form the acetyl radical (eq. [32]), which could subsequently recombine with a hydrogen atom to form acetaldehyde (eq. [33]). In addition, the radicals formed in equation (30) could be expected to subsequently recombine, yielding the vinyl alcohol molecule (eq. [34]). As stated, however, the reactions given in equations (30)–(34) all would require the formation of the vinyl radical and are therefore assumed not to be major pathways to these products in this experiment, since the vinyl radical was not observed in our experiments. It is also worth mentioning that we were unable to detect any absorptions of the oxirane

diradical intermediate H_2CCH_2O formed via reaction R3 (Fig. 2). This might actually suggest that the [1, 2]-H shift to acetaldehyde (eq. [27]), and possibly vinyl alcohol (eq. [28]) and/or the ring closure to ethylene oxide (eq. [26]), proceeds very rapidly within the time frame of a vibration period (typically 10^{-12} s). Finally, it is important to recall that we were able to fit the formation of the ethylene oxide column density via the reaction sequence (23) and (24); an involvement of a ring closure via the H_2CCH_2O diradical is not essential (sequence [26]), but cannot be ruled out as a minor contributor at this stage.

We now look closer at the dynamics and kinetics of reaction (23) followed by reactions (24)/(26), (27), and (25)/(28) to form ethylene oxide, acetaldehyde, and vinyl alcohol, respectively. Our investigations indicate that the formation of acetaldehyde [$k_3 = (8.5 \pm 0.3) \times 10^{-4}$ s^{-1}] is actually slightly *slower* than the synthesis of the ethylene oxide isomer [$k_4 = (1.1 \pm 0.1) \times 10^{-3}$ s^{-1}]. Since the formation of both isomers requires an initial addition of the oxygen atom to the carbon-carbon double bond of the ethylene molecule, the lower rate constant k_3 compared to k_4 could suggest that an additional reaction step is actually involved in the synthesis of acetaldehyde. This is very likely the [1, 2]-H shift of the H_2CCH_2O diradical. Therefore, the rate constants could verify the postulated reaction mechanism to form acetaldehyde via an addition of the oxygen atom to give a H_2CCH_2O diradical followed by a hydrogen shift; on the other hand, the ethylene oxide molecule could be formed in one step via addition of the oxygen atom to two carbon atoms simultaneously. It is also important to investigate the preexponential factors a and b in detail; the a/b ratio indicates the branching ratio of the synthesized acetaldehyde versus ethylene oxide isomers as the experimental time t approaches infinity. Recalling that $a = (4.0 \pm 2.7) \times 10^{15}$ cm^{-2} and $b = (4.3 \pm 3.6) \times 10^{15}$ cm^{-2}, this suggests that the column density ratio is close to unity. We established earlier that the preexponential factors can provide additional insight into the reaction mechanisms (Bennett et al. 2005); comparable preexponential factors suggest that the initial reaction step to form acetaldehyde and ethylene oxide may be involved a similar reaction mechanism, here the attack of the oxygen atom to the carbon-carbon double bond. This mechanism also helps us to understand the lower levels of detection of the third C_2H_4O isomer, vinyl alcohol. Here, the cone of acceptance of the π system of the ethylene molecule is actually *larger* than the cone of acceptance of the carbon-hydrogen σ bond (Levine & Bernstein 1987); recall that an insertion process into this bond is crucial to form vinyl alcohol, if it is formed by an insertion process (reaction R1, eq. [24], vs. reaction R2, eq. [25]). Recall that our experiments suggest lower column densities of vinyl alcohol compared to ethylene oxide and acetaldehyde—by a factor of 10. This also could support that the H_2CCH_2O diradical is not a crucial intermediate in the formation of vinyl alcohol. To summarize, both the rate constants as well as the preexponential factors verify that acetaldehyde, ethylene oxide, and vinyl alcohol are synthesized via reactions (23)–(28). However, we would like to stress that the actual involvement of the triplet versus singlet surface remains to be resolved. Briefly, ground-state oxygen atoms adding to ethylene have to overcome a barrier of a few kJ mol^{-1}, much larger than the averaged thermal energy of the ice matrix at 10 K. Therefore, reacting ground-state oxygen atoms need excess kinetic energy to overcome the entrance barrier. On the other hand, electronically excited oxygen atoms add and insert without barrier; however, thermal processes alone at 10 K can not supply this excitation energy. Therefore, these considerations underline the role of nonequilibrium chemistry (electronic excitation; excess kinetic energy) in the 10 K matrix.
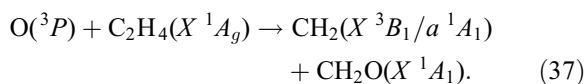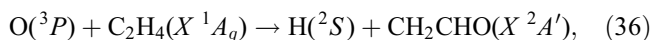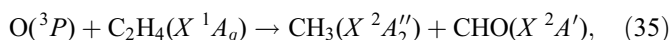
It is also important to examine the overall energetics of the reaction, first the liberation of an oxygen atom and second the actual formation of all three C_2H_4O isomers. Considering the column densities of the newly formed acetaldehyde, ethylene oxide, and vinyl alcohol isomers of $(3.3 \pm 1.7) \times 10^{15}$, $(4.2 \pm 3.8) \times 10^{15}$, and $(3.0 \pm 0.6) \times 10^{14}$ molecules cm^{-2}, respectively, about $(7.8 \pm 4.2) \times 10^{15}$ oxygen atoms cm^{-2} have to be generated via reactions (21) and (22); recalling that we are destroying $(1.1 \pm 0.1) \times 10^{17}$ molecules cm^{-2} of carbon dioxide, and that reactions (21) and (22) are solely responsible for the destruction of carbon dioxide, we still have $(1.0 \pm 0.1) \times 10^{17}$ oxygen atoms cm^{-2} unaccounted for. Using the same methodology for ethylene, we can conclude that $(1.1 \pm 0.5) \times 10^{17}$ molecules cm^{-2} are also unaccounted for, leading to the question as to what has happened to the remaining species. For the oxygen atoms, this can be answered fairly easily, since oxygen atoms can recombine with one another to give oxygen molecules (O_2), which would both be difficult to detect in our current setup, as we are limited to the detection of infrared-active species, and thus it is not expected for us to be able to account for these species. The possible detection of a minor contribution of ozone (O_3) and carbon trioxide (CO_3), as produced in experiments solely on carbon dioxide ices in this system (see Bennett et al. 2004), requires further investigation before quantitative contributions can be supplemented. Bear in mind that the carbon monoxide molecule (CO) cannot be used to account for the missing oxygen, because it is assumed to be generated concurrently with the oxygen atoms (see eqs. [21] and [22]), and so although it is observed as a first-order product, it is unlikely to account for these missing oxygen atoms, unless of course it is also produced in a higher order reaction. For the ethylene molecule, although we could not observe the vinyl radical, it is possible that a variety of C_xH_y chains/structures could be produced (1,3-butadiene [$CH_2CHCHCH_2$], for example, from the recombination of two vinyl radicals), which would consequently overlap with some of the ethylene fundamentals and remain difficult to assign unambiguously—again, this will be resolved in future experiments with labeled isotopes. It is also likely that ketene is produced in our experiment (especially if methylene [CH_2] radicals are produced in our experiment via destruction of the C-C π bond; note that the methylene radical itself is notoriously difficult to observe, see Yamaguchi et al. 1996)—the strongest absorption of ketene appearing at around 2144 cm^{-1} would appear close to the carbon monoxide fundamental at 2139 cm^{-1}, requiring further experimentation to resolve its presence, as several other bands also have conflicting overlaps with species detected in our experiments (see Schriver et al. 2004). If we account for the bond strength of the carbon-oxygen bond in carbon dioxide, about 1.3×10^{17} and 1.8×10^{17} eV are necessary to generate the atoms in their electronic ground and first excited states, respectively. Dynamic simulations using the CASINO code (Drouin et al. 2001) suggest that each 5 keV electron is fully absorbed within the ice sample within 600 nm, hence coupling a total of 4.4×10^{18} eV into the system. Therefore, only about 3%–4% of the kinetic energy of the electrons is consumed to generate oxygen atoms that reacted via equations (23)–(28) to form acetaldehyde, ethylene oxide, and vinyl alcohol; formally, reactions of ground-state oxygen atoms with an ethylene molecule are exoergic by 472, 354, and 429 kJ mol^{-1}, respectively.[7]

7. ASTROPHYSICAL IMPLICATIONS

Our detailed studies presented solid data on the synthesis of three C_2H_4O isomers in extraterrestrial ices, i.e., acetaldehyde,

---

[7] See http://webbook.nist.gov/chemistry.

ethylene oxide, and vinyl alcohol. The explicit detection of these isomers in electron-irradiated low-temperature carbon dioxide–ethylene ices at 10 K implies that energetic electrons generated by cosmic-ray particles via ionization of the target molecules in the "infra" track of the cosmic particle trajectory can be released perpendicularly to the ion path to actually synthesize acetaldehyde and ethylene oxide within the "ultra" track of the trajectory of the implant. Specifically, oxygen atoms were found to add to the carbon-carbon π bond of the ethylene molecule to form initially an oxirene diradical (addition to one carbon atom) or the cyclic ethylene oxide molecule (addition to two carbon atoms). The oxirene diradical can undergo a [1, 2]-H shift, forming the acetaldehyde and possibly vinyl alcohol molecules, or ring close to form ethylene oxide. Vinyl alcohol may also be produced by insertion of the oxygen atom into a carbon-hydrogen σ bond. Under gas-phase single-collision conditions of the same reaction, none of the C₂H₄O adduct molecules would survive; this is because the inherent high vibrational energy of the intermediates leads to a fragmentation via carbon-hydrogen and carbon-carbon bond ruptures, for which the major pathways involving reactions of ethylene with O (^3P) have been determined to be (1) dissociation into the methyl and formyl radicals (sequence [35]), (2) dissociation to the acetyl radical and a hydrogen atom (sequence [36]), and (3) dissociation to formaldehyde and the methylene radical (sequence [37]; Schmoltner et al. 1989):

$$O(^3P) + C_2H_4(X\ ^1A_g) \rightarrow CH_3(X\ ^2A_2'') + CHO(X\ ^2A'), \quad (35)$$

$$O(^3P) + C_2H_4(X\ ^1A_g) \rightarrow H(^2S) + CH_2CHO(X\ ^2A'), \quad (36)$$

$$O(^3P) + C_2H_4(X\ ^1A_g) \rightarrow CH_2(X\ ^3B_1/a\ ^1A_1) \\ + CH_2O(X\ ^1A_1). \quad (37)$$

Thus, both theoretical studies and crossed-beam experiments predict that the corresponding ethylene oxide and acetaldehyde molecules on the singlet surface are inaccessible due to the excess internal energy (rotational and/or vibrational), causing them to subsequently fragment (Schmoltner et al. 1989; Wortmann-Saleh et al. 1994; Belbruno 1997; Abou-Zied 1998; Gardner & Miller 2004). However, in the ice samples the internal energy of the intermediates can be diverted to the matrix via phonon coupling, thus stabilizing the ethylene oxide and acetaldehyde species. Similarly, in studies of O (^3P) with ethylene occurring in the liquid phase and high-pressure gas phase can also lead to stabilization of the intermediates, forming both ethylene oxide and acetaldehyde (Eusuf & Wagner 1972; Hirokami & Cvetanovic 1973; Bley et al. 1988). Note that a minor pathway to form ethylene oxide via ring closure of the oxirene diradical cannot be ruled out; likewise, the relative contributions of the triplet versus the singlet surfaces have to be investigated in future experiments.

Once acetaldehyde, ethylene oxide, and vinyl alcohol have been synthesized inside the ice layers of the coated grains in cold molecular clouds, the newly formed molecules can sublime as the cloud reaches the hot molecular core stage. It is often noted that ices such as these may not be relevant to interstellar ices based on the consideration that we require CO₂ and CH₄ (to produce C₂H₄) as being present next to each other within these ices. However, we would like to stress that the carbon dioxide molecule does not present an essential reactant molecule; any oxygen-bearing molecule such as carbon monoxide or water might be considered also as a potential oxygen atom reservoir, as long as this oxygen atom can be released efficiently via cosmic-ray particles deep inside cold molecular clouds. It is difficult to derive a quantitative extrapolation for how our present experiments are relevant to the production of these molecules in interstellar grains, as it is noted that the ice mixture of our experiments is not representative of that of an interstellar ice—it is also noted that the initial composition of the ices can have an effect on the UV destruction of molecules (Cottin et al. 2003) and the production of new molecules in the ion irradiation of ices (Satorre et al. 2000). In order to quantify the importance of these reactions in the interstellar medium, we need to carry out further experiments that investigate how the initial reaction mixture affects the reaction pathways—this includes varying the ratios of carbon monoxide and ethylene, as well as the inclusion of additional molecules that are more representative of interstellar ices mixtures (i.e., water, carbon monoxide, etc.).

In conclusion, it is important to compare these laboratory studies with actual astronomical investigations. Here, we identified two routes to form acetaldehyde in carbon monoxide–methane (Bennett et al. 2005) and in carbon dioxide–ethylene mixtures; on the other hand, ethylene oxide and vinyl alcohol were solely found in irradiated carbon dioxide–ethylene samples. Since only carbon monoxide, carbon dioxide, and methane have been observed in interstellar ices (Lacy et al. 1984, 1991; Tielens et al. 1991; Boogert et al. 1996, 1997; Gerakines et al. 1999; Fraser et al. 2002; Gibb et al. 2004)—ethylene is formed as a secondary product by charged particle irradiation and photolysis of methane ices and is likely present at hitherto unobservable concentrations of less than 1% on interstellar grains—if we assume that the relative production rates of acetaldehyde and ethylene oxide would be similar in a more astrophysically relevant ice mixture, we would expect that in hot molecular cores the fractional abundances of acetaldehyde are higher than those of ethylene oxide. This hypothesis gains strong support from Ikeda et al. (2001). The authors observed both acetaldehyde and ethylene oxide toward massive star-forming regions. First, the observed abundances of both isomers are a factor of 2–600 higher than predicted from pure gas-phase models, suggesting that solid-state processes indeed play an important role in their formation (Charnley 2004). Second, the abundance of acetaldehyde was found to be systematically higher than that of ethylene oxide by a factor of 1.2–13.2. Similar ratios of 2.5–10 toward hot cores were given by Nummelin et al. (1998), suggesting that our laboratory studies, which are computed to simulate about 10^6 yr of radiation exposure of interstellar ices, i.e., a typical lifetime of a cold molecular cloud, can indeed predict the trends of an enhanced acetaldehyde production, as compared to ethylene oxide. It should be noted, however, that there could be a strong temperature dependence on the formation routes of C₂H₄O isomers within interstellar grains before their subsequent release into the gas phase in these regions *if* thermalized oxygen atoms react via intersystem crossing, too. However, our findings suggest that *if* the reaction of oxygen atoms with ethylene is the only source of ethylene oxide and vinyl alcohol, the latter should be less abundant by a factor of 10 in hot cores. This contradicts the astronomical observations, which suggest a ratio of about 1.5. Therefore, the reaction of oxygen atoms with ethylene cannot be the sole source to form vinyl alcohol on interstellar ices. One additional route might be the involvement of the water-acetylene system (Hudson & Moore 2003), in which vinyl alcohol can be formed upon exposure to ionizing radiation, too. Our laboratory experiments also propose that acetaldehyde might be indeed the carrier of the 1349 cm⁻¹ CH deformation mode (7.414 μm) observed toward interstellar ices (Gibb et al. 2004), where abundances of ~9% (relative to water) have been reported for the high-mass young stellar objects W33A and AFGL 7009S. Similar synthetic routes could help explain the formation

of acetaldehyde and ethylene oxide in comet C/1995 O1 (Hale-Bopp), as postulated by Crovisier et al. (2004). Finally, Bernard et al. (2003) detected ethylene oxide in gas discharge experiments simulating the charged particle processing of Titan's atmosphere. Here, carbon monoxide—a precursor to atomic oxygen—and the ethylene reactant were detected in Titan's atmosphere at mixing ratios of up to 10^{-4} and 2×10^{-7}, respectively. If the reaction of liberated oxygen atoms with ethylene takes place in those atmospheric layers where three-body processes frequently occur, the ethylene oxide intermediate can be stabilized by collision with a "bath" molecule. Surprisingly, the ethylene oxide molecule was found to be produced in preference to the predicted formaldehyde and methanol molecules when modeling Titan's atmosphere (Coll et al. 2003). To summarize, laboratory experiments like the present study provide valuable constraints on theories in astrochemistry and supply valuable information on the importance of charged particle processing of complex organic molecules in extraterrestrial environments. Future investigations on this system will reinvestigate the formation of the vinyl alcohol isomer—here via energetic electron processing of acetylene-water matrices, to compare the findings with Hudson & Moore (2003)—and will also focus on the theoretical investigation of the complete triplet and singlet C_2H_4O surfaces, including the calculation of intersystem crossing rate constants.

REFERENCES

Abou-Zied, O. K., & McDonald, J. D. 1998, J. Chem. Phys., 109, 1293
Allamandola, L. J., Bernstein, M. P., Sandford, S. A., & Walker, R. L. 1999, Space Sci. Rev., 90, 219
Basiuk, V. A., & Kobayashi, K. 2004, Int. J. Quantum Chem., 97, 713
Becke, A. D. 1993, J. Chem. Phys., 98, 5648
Belbruno, J. J. 1997, J. Phys. Organic Chem., 10, 113
Bell, M. B., Matthews, H. E., & Feldman, P. A. 1983, A&A, 127, 420
Bennett, C. J., Jamieson, C. S., Mebel, A. M., & Kaiser, R. I. 2004, Phys. Chem. Chem. Phys., 6, 735
Bennett, C. J., Jamieson, C. S., Osamura, Y., & Kaiser, R. I. 2005, ApJ, 624, 1097
Bernard, J. M., Coll, P., Coustenis, A., & Raulin, F. 2003, Planet. Space Sci., 51, 1003
Bernstein, M. P., Dworkin, J. P., Sandford, S. A., Cooper, G. W., & Allamandola, L. J. 2002, Nature, 416, 401
Bley, U., Dransfield, P., Himme, B., Koch, M., Temps, F., & Wagner, H. G. 1988, in Proc. 22nd Symposium on Combustion (Pittsburgh: Combustion Inst.), 997
Bohn, R. B., Sandford, S. A., Allamandola, L. J., & Cruikshank, D. P. 1994, Icarus, 111, 151
Boogert, A. C. A., Helmich, F. P., van Dishoeck, E. F., Schutte, W. A., Tielens, A. G. G. M., & Whittet, D. C. B. 1998, A&A, 336, 352
Boogert, A. C. A., Schutte, W. A., Helmich, F. P., Tielens, A. G. G. M., & Wooden, D. H. 1997, A&A, 317, 929
Boogert, A. C. A., et al. 1996, A&A, 315, L377
Brucato, J. R., Palumbo, M. E., & Strazzulla, G. 1997, Icarus, 125, 135
Caselli, P., Hasegawa, T. I., & Herbst, E. 1993, ApJ, 408, 548
Charnley, S. B. 2004, Adv. Space Res., 33, 23
Charnley, S. B., & Markwick, A. J. 2003, A&A, 399, 583
Charnley, S. B., Rodgers, S. D., & Ehrenfreund, P. 2001, A&A, 378, 1024
Charnley, S. B., Tielens, A. G. G. M., & Millar, T. J. 1992, ApJ, 399, L71
Cleaves, H. J., II. 2003, Monatshefte Chem., 134, 585
Coll, P., Bernard, J.-M., Navarro-González, R., & Raulin, F. 2003, ApJ, 598, 700
Cottin, H., Moore, M. H., & Bénilan, Y. 2003, ApJ, 590, 874
Crovisier, J. 1998, Faraday Discuss., 109, 437
Crovisier, J., Bockelée-Morvan, D., Colom, P., Biver, N., & Despois, D. 2004, A&A, 418, 1141
Dartois, E., Demyk, K., d'Hendecourt, L., & Ehrenfreud, P. 1999, A&A, 351, 1066
d'Hendecourt, L., Jourdain de Muizon, M., Dartois, E., Demyk, K., Ehrenfreund, P., & Heras, A. 1999, in The Universe as Seen by ISO, ed. P. Cox & M. F. Kessler (ESA SP-427; Noordwijk: ESA), 589
Dickens, J. E., Irvine, W. M., Ohishi, M., Ikeda, M., Isikawa, S., Nummelin, A., & Hjalmarson, Å. 1997, ApJ, 489, 753
Donnay, J. D. H., & Ondik, H. M. 1972, Crystal Data: Determinative Tables, Vol. 1 (3rd ed.; Washington: NBS)
Draine, B. T. 2003, ARA&A, 41, 241
Drouin, D., Couture, A. R., Gauvin, R., Hovington, P., Horny, P., & Demers, H. 2001, Monte Carlo Simulation of Electron Trajectory in Solids (CASINO) (ver. 2.42; Sherbrooke: Univ. Sherbrooke)
Dunning, T. H. 1989, J. Chem. Phys., 90, 1007
Ehrenfreund, P., Boogert, A. C. A., Gerakines, P. A., Jansen, D. J., Schutte, W. A., Tielens, A. G. G. M., & van Dishoeck, E. F. 1996, A&A, 312, 263
Ehrenfreund, P., d'Hendecourt, L., Dartois, E., Jourdain de Muizon, M., Breitfellner, M., Puget, J. L., & Habing, H. J. 1997, Icarus, 130, 1

Ehrenfreund, P., Kraft, C., Kochan, H., & Pironello, V., eds. 1998, Laboratory Astrophysics and Space Research (Dordrecht: Kluwer)
Ehrenfreund, P., & Schutte, W. A. 2000, in IAU Symp. 197, Astrochemistry: From Molecular Clouds to Planetary Systems, ed. Y. C. Minh & E. F. van Dishoeck (San Francisco: ASP), 135
El-Nawawy, M. S., Howe, D. A., & Millar, T. J. 1997, MNRAS, 292, 481
Eusuf, M., & Wagner, H. G. 1972, Ber. Bunsengesch. Phys. Chem., 76, 444
Fairley, D. A., Scott, G. B. I., Freeman, C. G., Maclagan, R. G. A. R., & McEwan, M. J. 1996, J. Chem. Soc. Faraday Trans., 92, 1305
Fourikis, N., Sinclair, M. W., Robinson, B. J., Godfrey, P. D., & Brown, R. D. 1974, Australian J. Phys., 27, 425
Fraser, H. J., McCoustra, M. R. S., & Williams, D. A. 2002, Astron. Geophys., 43(2), 10
Frisch, M. J., et al. 2001, Gaussian 98 (rev. A.9; Pittsburgh: Gaussian, Inc.)
Gardner, J. L., & Miller, S. G. 2004, J. Chem. Phys., 121, 5920
Gerakines, P. A., Moore, M. H., & Hudson, R. L. 2004, Icarus, 170, 202
Gerakines, P. A., Schutte, W. A., & Ehrenfreund, P. 1996, A&A, 312, 289
Gerakines, P. A., Schutte, W. A., Greenberg, J. M., & van Dishoeck, E. F. 1995, A&A, 296, 810
Gerakines, P. A., et al. 1999, ApJ, 522, 357
Gibb, E., Nummelin, A., Irvine, W. M., Whittet, D. C. B., & Bergman, P. 2000, ApJ, 545, 309
Gibb, E. L., Whittet, D. C. B., Boogert, A. C. A., & Tielens, A. G. G. M. 2004, ApJS, 151, 35
Hartquist, T. H., & Williams, D. A., eds. 1998, The Molecular Astrophysics of Stars and Galaxies (Oxford: Clarendon)
Hawkins, M., & Andrews, L. 1983, J. Am. Chem. Soc., 105, 2523
Hirokami, S., & Cvetanovic, R. J. 1973, Canadian J. Chem., 51, 373
Hjalmarson, Å., Bergman, P., & Nummelin, A. 2001, in Exo-/Astro-Biology, ed. P. Ehrenfreund, O. Angerer, & B. Battrick (ESA SP-496; Noordwijk: ESA), 263
Hollis, J. M., Lovas, F. J., & Jewell, P. R. 2000, ApJ, 540, L107
Hudson, R. L., & Moore, M. H. 1999, Icarus, 140, 451
———. 2003, ApJ, 586, L107
Huntress, W. T., & Mitchell, G. F. 1979, ApJ, 231, 456
Ikeda, M., Ohishi, M., Nummelin, A., Dickens, J. E., Bergman, P., Hjalmarson Å., & Irvine, W. M. 2001, ApJ, 560, 792
Johnson, R. E. 1990, Energetic Charged Particle Interactions with Atmospheres and Surfaces (Berlin: Springer)
———. 1996, Rev. Mod. Phys., 68, 305
Kaiser, R. I. 2002, Chem. Rev., 102, 1309
Kaiser, R. I., Eich, G., Gabrysch, A., & Roessler, K. 1999, A&A, 346, 340
Kaiser, R. I., Gabrysch, A., & Roessler, K. 1995, Rev. Sci. Instrum., 66, 3058
Kaiser, R. I., & Roessler, K. 1997, ApJ, 475, 144
———. 1998, ApJ, 503, 959
Keane, J. V., Tielens, A. G. G. M., Boogert, A. C. A., Schutte, W. A., & Whittet, D. C. B. 2001, A&A, 376, 254
Kuan, Y.-J., Charnley, S. B., Huang, H.-C., Kisiel, Z., Ehrenfreund, P., Tseng, W.-L., & Yan, C.-H. 2004, Adv. Space Res., 33, 31
Kuan, Y.-J., Charnley, S. B., Huang, H.-C., Tseng, W. L., & Kisiel, Z. 2003, ApJ, 593, 848
Lacy, J. H., Baas, F., Allamandola, L. J., Persson, S. E., McGregor, P. J., Lonsdale, C. J., Geballe, T. R., & van de Bult, C. E. P. 1984, ApJ, 276, 533
Lacy, J. H., Carr, J. S., Evans, N. J., II, Baas, F., Achtermann, J. M., & Arens, J. F. 1991, ApJ, 376, 556

Lécluse, C., Robert, F., Kaiser, R. I., Roessler, K., Pillinger, C. T., & Javoy, M. 1998, A&A, 330, 1175

Lee, C., Yang, W., & Parr, R. G. 1988, Phys. Rev. B, 37, 785

Leung, C. M., Herbst, E., & Huebner, W. F. 1984, ApJS, 56, 231

Levine, R. D., & Bernstein, R. B. 1987, Molecular Reaction Dynamics and Chemical Reactivity (Oxford: Oxford Univ. Press)

Matthews, H. E., Friberg, P., & Irvine, W. M. 1985, ApJ, 290, 609

Millar, T. J. 2002, Planet. Space Sci., 50, 1189

Millar, T. J., & Hatchell, J. 1998, Faraday Discuss., 109, 15

Millar, T. J., Macdonald, G. H., & Gibb, A. G. 1997, A&A, 325, 1163

Miller, S. L., & Schlesinger, G. 1993, J. Mol. Evolution, 36, 302

Minh, Y. C., & van Dishoeck, E. F., ed. 2000, IAU Symp. 197, Astrochemistry: From Molecular Clouds to Planetary Systems (San Francisco: ASP)

Muñoz Caro, G. M., & Schutte, W. A. 2003, A&A, 412, 121

Nomura, H., & Millar, T. J. 2004, A&A, 414, 409

Nummelin, A., Dickens, J. E., Bergman, P., Hjalmarson Å., Irvine, W. M., Ikeda, M., & Ohishi, M. 1998, A&A, 337, 275

Palumbo, M. E., Castorina, A. C., & Strazzulla, G. 1999, A&A, 342, 551

Palumbo, M. E., Pendleton, Y. J., & Strazzulla, G. 2000, ApJ, 542, 890

Pendleton, Y. V. 1997, Origins Life Evol. Biosphere, 27, 53

Price, R. J., Viti, S., & Williams, D. A. 2003, MNRAS, 343, 1257

Purvis, G. D., & Bartlett, R. J. 1982, J. Chem. Phys., 76, 1910

Rae, J. G. L., Green, N. J. B., Hartquist, T. W., Pilling, M. J., & Toniazzo, T. 2003, A&A, 405, 387

Raghavachari, K., Trucks, G. W., Pople, J. A., & Head-Gordon, M. 1989, Chem. Phys. Lett., 157, 479

Rodgers, S. D., & Charnley, S. B. 2003, ApJ, 585, 355

Roessler, K. 1992, Nucl. Instrum. Methods Phys. Res. B, 65, 55

Ruffle, D. P., & Herbst, E. 2001, MNRAS, 322, 770

Sandford, S. A., Allamandola, L. J., Tielens, A. G. G. M., & Valero, G. J. 1988, ApJ, 329, 498

Satorre, M. A., Palumbo, M. E., & Strazzulla, G. 2000, Ap&SS, 274, 643

Schmoltner, A. M., Chu, P. M., Brudzynski, R. J., & Lee, Y. T. 1989, J. Chem. Phys., 91, 6926

Schriver, A., Coanga, J. M., Schriver-Mazzouli, L., & Ehrenfreund, P. 2004, Chem. Phys., 303, 13

Schutte, W. A. 1998, in Laboratory Astrophysics and Space Research, ed. P. Ehrenfreud et al. (Dordrecht: Kluwer), 69

Shimanouchi, T. 1972, Tables of Molecular Vibrational Frequencies, Consolidated Vol. I (Washington: NBS)

Smith, D., & Adams, N. G. 1977, ApJ, 217, 741

Smith, M. B., & March, J. 2001, March's Advanced Organic Chemistry: Reactions, Mechanisms, and Structure (5th ed.; New York: Wiley)

Smith, R., ed. 1997, Atomic and Ion Collisions in Solids and at Surfaces (Cambridge: Cambridge Univ. Press)

Stantcheva, T., Caselli, P., & Herbst, E. 2001, A&A, 375, 673

Strazzulla, G., & Palumbo, M. E. 1998, Planet. Space Sci., 46, 1339

Tielens, A. G. G. M., Tokunage, A. T., Geballe, T. R., & Baas, F. 1991, ApJ, 381, 181

Turner, B. E. 1991, ApJS, 76, 617

Turner, B. E., & Apponi, A. J. 2001, ApJ, 561, L207

Turner, B. E., Terzieva, R., & Herbst, E. 1999, ApJ, 518, 699

Wiebe, D., Semenov, D., & Henning, T. 2003, A&A, 399, 197

Williams, D. A., & Hartquist, T. W. 1999, Accounts Chem. Res., 32, 334

Williams, D. A., & Herbst, E. 2002, Surface Sci., 500, 823

Wortmann-Saleh, D., Engels, B., & Peyerimhoff, S. D. 1994, J. Phys. Chem., 98, 9541

Yamaguchi, Y., Sherrill, C. D., & Schaefer, H. F., III. 1996, J. Phys. Chem., 100, 7911

Zhitnikov, R. A., & Dmitriev, Y. A. 2002, A&A, 386, 1129

Ziurys, L. M., & McGonagle, D. 1993, ApJS, 89, 155